A. K. Hagenlocher
W. T. Chen

Space-charge-limited Current Instabilities in n^+-π-n^+ Silicon Diodes

Abstract: If the strength of a pulsed electric field of about 10^3 volts/cm is exceeded in a nickel-doped 25,000 ohm-cm π-type silicon sample with n^+ contacts, a transient charge distribution is established that leads to a current instability. When the critical applied field is reached a current-controlled negative resistance is observed. The sample impedance decreases by several orders of magnitude, with a switching time in the nanosecond range, and microwave oscillations are produced. Below the threshold a space-charge-limited current flows, and voltage profile measurements show the presence of the expected negative space charge near the cathode. As the field is increased this space charge extends further into the sample. At the threshold the nickel centers become ionized, and a positive space charge is created in the center of the sample. This non-equilibrium distribution, which persists for a period of 200 to 300 microseconds, has properties similar to those of a gaseous plasma.

Introduction

A long-lasting transient instability leading to an S-shaped current-voltage characteristic is observed in high-resistivity nickel-doped p-type silicon preceding the steady-state space-charge-limited current conditions. Whereas steady-state single- and double-carrier injection phenomena leading to space- charge-limited currents (SCLC) were reported in theory[1-4] and experiments,[5-8] there is little theoretical understanding for the various instabilities which may occur in connection with SCLC.

The instability observed in nickel-doped 25,000 ohm-cm silicon leads to a bistable condition which switches the sample at a threshold voltage from a high- to a low-impedance state. This effect occurs only if a two-carrier SCLC is present which is generated by injection into the contacts and by impact ionization of the nickel atoms within the sample. Ghandi, Mortenson and Park[11] have demonstrated the capability of impact ionization of nickel impurity centers in silicon; however, their device worked under ohmic rather than SCLC conditions, and their results are, therefore in many aspects, different from the one reported here.

Approach to the problem

Two n^+ layers are used as contacts on the π-type silicon. The cathode is an injecting contact for electrons whereas the second contact has blocking properties at low field strength. When the field is increased, the anode operates under punch-through conditions and allows holes to enter the sample from the other side. The number of injected electron and holes is not the same in this configuration; however, the cube relation between current and voltage is observed which is typical for double injection, but the current flow is considerably lower than for double injection in an n^+-π-p^+ diode. Higher injection levels cause a negative current-controlled resistance regime. This is also observed for an n^+-π-n^+ structure at a threshold voltage of about 5×10^4 V/cm. This threshold can be lowered by at least one order of magnitude in nickel-doped silicon by generating additional carriers within the bulk of the specimen.

Preparation of the specimen

Lapped silicon slices of a resistivity of 45,000 ohm-cm p-type, 500μ thick, are used as starting material. Nickel is diffused into the silicon from both sides at temperatures ranging from 1050° to 1150°C over a period of 2 to 5 hours. A slice is then polished to the thickness required for the sample; this varied for the experiments from 50 to 250μ. An n^+-layer about 3μm deep (an electrode) is formed on both surfaces in an atmosphere of phosphorus oxychloride, argon and oxygen at 1050°C. The slice is diced, wires are bonded to the contacts and the diode packaged. The standard size used was 2000 × 2000 × 125 μm.

By the nickel doping the resistivity dropped to 20,000–

The authors are with the Bayside Research Center of the General Telephone and Electronics Laboratories Incorporated, Bayside, New York 11360.

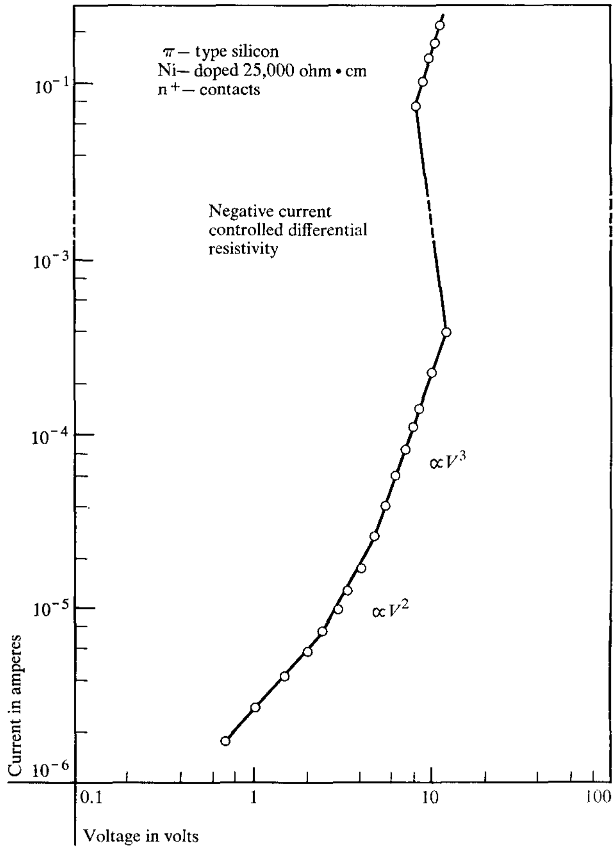

Figure 1 Current versus voltage characteristic of a n^+-π(Ni)-n^+ silicon diode.

25,000 ohm-cm. This corresponds to an nickel concentration of 10^{13} to 10^{14} per cm^3 for electrically active centers. But since nickel precipitates on dislocations where it is electrically inactive, the actual nickel content should be approximately 10^{17} per cm^3 according to Tokomaru.[12]

Bistable condition

The n^+-π(Ni)-n^+ diodes show a negative current-controlled resistivity above a threshold voltage V_{th}. This phenomenon is represented by a bistable condition in which the sample changes from a high- to a low-impedance state. Samples are reproducible if processed together and the variation of threshold voltage with the contact distance is then nearly linear. On the other hand, there is still no consistency in the number of electrically active nickel atoms generated if different diffusion cycles are compared. This explains the variation of the threshold field strength from 800 to 6000 volts/cm on the individual sample. The change from the high- to the low-impedance state may be a factor between 10^1 and 10^4, but its magnitude also depends strongly on the external circuit impedance. There is no hysteresis observed between the two switching directions. The switching time from the high- to the low-impedance state and vice versa is vary fast; it is below the resolution time of the equipment, which is 10^{-8} sec. To avoid heating of the diode, pulses of 5 to 250 μsec duration were used for the measurements. At the beginning of a pulse there is a delay of 50 to 200 nsec. Since this time agrees closely with the transit time of the carriers, the delay time is believed to be transit-time originated. The S-shaped characteristic can be observed properly only if SCLC conditions are established preceding V_{th}. Figure 1 shows the typical behavior of a diode having a contact distance of 125μm. At low fields the diode follows Ohm's Law. This region is succeeded by a square or near-square relation with an increasing field strength, and shows that excess electrons are injected. The threshold voltage for the square dependence is only half of that predicted for the single carrier majority space charge.[13] However, it is several orders of magnitude too low for the V^2 relation in the case of double injection with the transit time still larger than the dielectric relaxation time. If the current density J is expressed for a sample of the length L at the voltage V by

$$J = AV^2/L^3, \quad (1)$$

the constant A is about 10^{-10} [A-cm/V^2] for the n^+-π-n^+ diodes, whereas it is four orders of magnitude larger for the long samples reported by Marsh, Mayer and Baron.[14] The length of their samples is large compared with the ambipolar diffusion length. This is not the case for the diode used in this study. The V^3-relation starts when punch-through conditions are reached at the anode. Further increase of the voltage multiplies the number of carriers and drives the specimen through an unstable region into the low-impedance state. It may be mentioned that the sample is now very close to the value that Lampert[1] predicts for double injection in an insulator. In order to obtain the instabilities with a fast switching time and no hysteresis, the cube current versus voltage relation has to precede the S-shaped characteristic. The characteristic above the bistable condition is much too dependent on the impedance of the power source to give any explanation.

The switching from the high- to low-impedance state is not observed reproducibly in p^+-π(Ni)-p^+ or p^+-π(Ni)-n^+ structures. When it does occur, it is not as well defined as in the n^+-π(Ni)-n^+ samples.

Okazaki and Hiramatsu[10] also found a square and cube current-voltage relationship for their short samples of 0.15 mm length under SCLC conditions.

Oscillations

The instabilities above the threshold voltage lead to microwave oscillations if the diode is placed in a microwave circuit and biased above V_{th}. Figure 2 shows the diagram of the measuring equipment. The device is packaged in a 1N23 cartridge. The diodes are operated with pulses of 500 nsec in length and a repetition rate of 100 Hz. For these experiments samples with a threshold voltage higher than that shown in Fig. 1 were selected. A typical frequency is 1.68 GHz at an output power of 2W, with an efficiency of 0.2% at 60 volts and 16.5 amperes. The heat transfer from the sample is poor and an arrangement for better cooling would probably upgrade the efficiency. By using a resonant cavity the frequency can be tuned over 30%. Oscillations under SCLC conditions were reported by Holonyak, Kikuchi and others.[15–19] However, the frequencies are in the kilocycle or megacycle range.

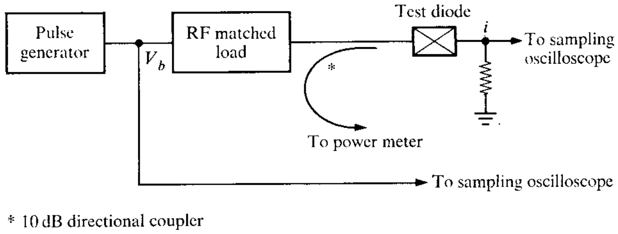

Figure 2 Nonresonant circuit for rf evaluation of test diode.

Figure 3 Potential profile across a diode.

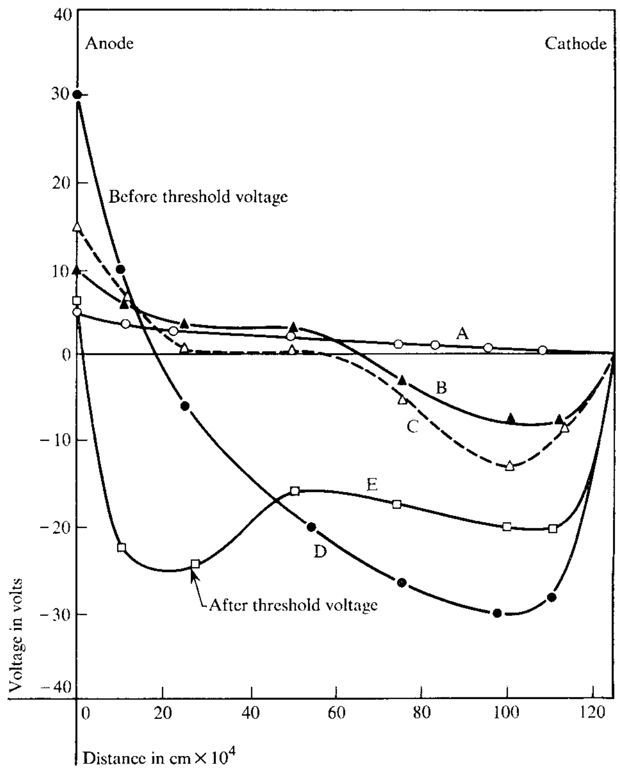

Voltage and charge profile

Measurements on samples of different widths indicate that a bulk effect is responsible for the instabilities. The need for nickel doping over the whole sample supports this conclusion. This bulk effect would mean that at a relatively uniform field distribution the field strength at the threshold voltage would be very low compared with avalanche diode or Gunn oscillations. In order to determine if there are any localized high-field areas, the voltage profile of the silicon structures was measured. This experiment showed a long-lasting transient field and charge distribution over a period of 200 to 300 μsec until a distribution to the steady-state condition was obtained. During this time large localized space charge can generate high internal fields.

The potential distribution measurements were made by pressing a probe against the polished surface of the silicon; alloyed contacts were also used. Both methods showed a qualitative agreement, but due to the relatively large part of the sample covered by an alloyed connection, the maximum potential values observed with a thin probe were much higher than on an alloyed contact. Figure 3 shows the voltage profile of a sample with $V_{th} = 30$ volts taken 10 μsec after the start of a pulse. The curves should be considered as a qualitative picture since it was difficult to obtain an accurate measurement of position and voltage. Curve A has the lowest field strength applied and represents an ohmic distribution. After the voltage is increased to 10 volts (curve B), an accumulation of negative charges is seen at the cathode caused by electron injection. This space charge makes the area inside the sample close to the cathode more negative than the cathode. With increasing applied voltage the negative space charge extends further into the sample. When the threshold voltage is reached (curve D), the negative space charge covers 80% of the specimen. After the sample switches into the low-impedance state (curve E), a sharp drop in the voltage starts at the anode, but little change occurs compared with curve D over a large part of the sample. These measurements show the existence of large internal fields which, over parts of the sample, exceed and oppose the externally applied field. A similar appearance is reported by Bullis[20] for a gas plasma in a thermionic converter. The excess charge density can be evaluated from Fig. 3 by applying Poisson's equation

$$\frac{d^2 V}{dx^2} = \frac{-(N - P)e}{\epsilon}, \qquad (2)$$

where N and P are the total negative and positive charge, mobile and fixed. The result is shown in Fig. 4 for the two most interesting cases, before and after the switching. At V_{th} an excess of negative charge appears with a concentration of about 10^{13} per cm^3. There are two peaks in the distribution, the larger lying close to the cathode.

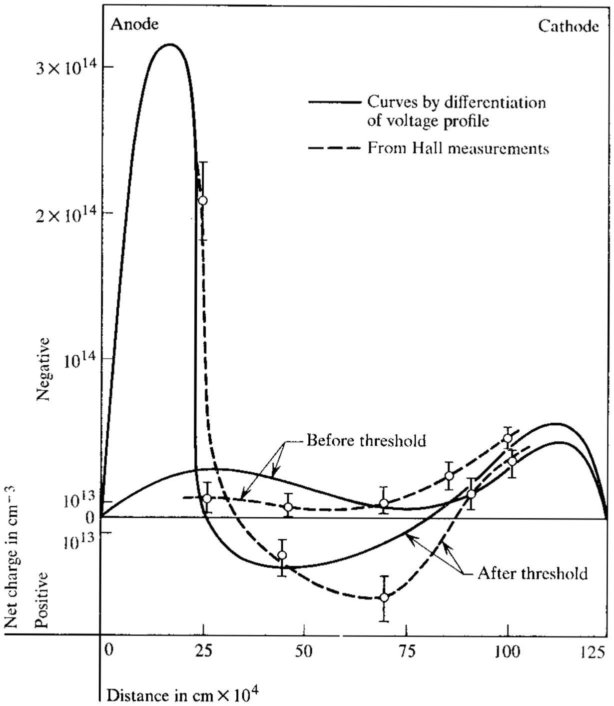

Figure 4 Charge profile of a sample before and after the threshold voltage has been applied.

In the low-impedance state an additional large accumulation of negative charges is observed close to the anode, whereas in the center section positive charges are dominating. Therefore two junction-like transitions appear on both sides of the center of the sample. This is confirmed qualitively by Hall measurements which are also shown in Fig. 4. It can therefore be concluded that mobile charges are largely responsible for the profile.

A simple experiment confirms that the center section is the most critical part responsible for the instabilities. A probe connected through a 10-megohm resistor to the anode reduces V_{th} by 1 volt if pressed against the critical area, whereas no change is observed if contact is made to other parts of the silicon. Using the Suhl effect together with different surface conditions, the effective lifetime can be reduced by a magnetic field. Since the V^3 dependence of double injection SCLC is dependent on the lifetime, the current changes at constant voltage with the magnetic field. V_{th} is also influenced and the oscillation can be augmented or quenched depending upon whether the carriers are driven by the magnetic field to a surface with larger or smaller surface recombination velocity. This experiment strongly suggests that the instability is not caused by filament formation.

Conclusions

The instability in high-resistivity, nickel-doped silicon is generated by a transient distribution of space charges with a duration of 200 to 300 μsec. During this period large internal electric fields form which exceed the externally applied field. An injection of electrons and holes is required, but it appears that their concentrations are not equal as in the case of the common double-injection SCLC. The contact distance is of the same order of magnitude as the ambipolar diffusion length; nevertheless, the typical square and cube current-voltage relations for SCLC are observed. There is no evidence that a trapping mechanism is originated by the nickel atoms which has influence on the dc characteristic.

Acknowledgments

We want to thank M. S. Wasserman for support of this study and for numerous discussions; D. Fleri and R. I. Harrison for valuable suggestions, and F. Ryder for his excellent work in preparing the samples.

References

1. M. A. Lampert, *Phys. Rev.* **125,** 126 (1962).
2. M. A. Lampert, *RCA Rev.* **20,** 682 (1959).
3. R. H. Parmenter and W. Ruppel, *J. Appl. Phys.* **30,** 548 (1959).
4. A. Rose, *J. Appl. Phys.* **35,** 2664 (1964).
5. N. Holonyak, *Proc. IRE* **50,** 2421 (1962).
6. R. Baron, J. W. Mayer and O. J. Marsh, *Appl. Phys. Letters* **4,** 65 (1964).
7. J. W. Mayer, R. Baron and O. J. Marsh, *Phys. Rev.* **137A,** 286 (1965).
8. J. W. Mayer, R. Baron and O. J. Marsh, *J. Appl. Phys.* **39,** 1447 (1968).
9. G. T. Wright, *Solid State Electronics* **5,** 117 (1962).
10. S. Okazaki and M. Hiramatsu, *J. Appl. Phys. (Japan)* **7,** 557 (1968).
11. S. K. Ghandi, K. E. Mortenson and J. N. Park, *IEEE Trans. Elec. Devices* **13,** 515 (1966).
12. Y. Tokomaru, *J. Appl. Phys. (Japan)* **2,** 542 (1963).
13. N. F. Mott and R. W. Gurney, *Electronic Processes in Ionic Crystals,* Oxford University Press, New York 1940, 1st ed., p. 172.
14. O. J. Marsh, J. W. Mayer and R. Baron, *Appl. Phys. Letters* **4,** 74 (1964).
15. N. Holonyak, Jr. and S. F. Bevacqua, *Appl. Phys. Letters* **2,** 71 (1963).
16. J. S. Moore, N. Holonyak, Jr., M. D. Sirkis and M. M. Blouke, *Appl. Phys. Letters* **2,** 58 (1963).
17. J. S. Moore, C. M. Penchina, N. Holonyak, Jr., M. D. Sirkis and T. Yamada, *J. Appl. Phys.* **37,** 2009 (1966).
18. M. Kikuchi, *J. Appl. Phys.* **37,** 4285 (1966).
19. J. S. Moore, N. Holonyak, Jr. and M. D. Sirkis, *Solid State Electronics* **10,** 823 (1967).
20. R. H. Bullis, L. K. Hansen, C. Warner, J. M. Houston, M. F. Koskinen and N. S. Rasor, *J. Appl. Phys.* **38,** 3425 (1967).

Received April 17, 1969